

# A peptide encoded within a 5' untranslated region promotes pain sensitization in mice

Paulino Barragan-Iglesias<sup>a,b</sup>, Nikesh Kunder<sup>c</sup>, Andi Wangzhou<sup>a</sup>, Bryan Black<sup>d</sup>, Pradipta R. Ray<sup>a</sup>, Tzu-Fang Lou<sup>c</sup>, June Bryan de la Peña<sup>c</sup>, Rahul Atmaramani<sup>d</sup>, Tarjani Shukla<sup>c</sup>, Joseph J. Pancrazio<sup>d,e</sup>, Theodore J. Price<sup>a,e</sup>, Zachary T. Campbell<sup>c,e,\*</sup>

## Abstract

Translational regulation permeates neuronal function. Nociceptors are sensory neurons responsible for the detection of harmful stimuli. Changes in their activity, termed plasticity, are intimately linked to the persistence of pain. Although inhibitors of protein synthesis robustly attenuate pain-associated behavior, the underlying targets that support plasticity are largely unknown. Here, we examine the contribution of protein synthesis in regions of RNA annotated as noncoding. Based on analyses of previously reported ribosome profiling data, we provide evidence for widespread translation in noncoding transcripts and regulatory regions of mRNAs. We identify an increase in ribosome occupancy in the 5' untranslated regions of the calcitonin gene-related peptide (CGRP/*Calca*). We validate the existence of an upstream open reading frame (uORF) using a series of reporter assays. Fusion of the uORF to a luciferase reporter revealed active translation in dorsal root ganglion neurons after nucleofection. Injection of the peptide corresponding to the calcitonin gene-related peptide–encoded uORF resulted in pain-associated behavioral responses in vivo and nociceptor sensitization in vitro. An inhibitor of heterotrimeric G protein signaling blocks both effects. Collectively, the data suggest pervasive translation in regions of the transcriptome annotated as noncoding in dorsal root ganglion neurons and identify a specific uORF-encoded peptide that promotes pain sensitization through GPCR signaling.

**Keywords:** uORF, Nociceptor plasticity, *Calca*/CGRP, Pain, Translational control, Peptide

## 1. Introduction

Translational regulation pervades neuronal plasticity.<sup>21,51</sup> mRNAs possess 2 untranslated regions that flank the coding sequence—the 5' and 3' untranslated region (UTR). Both serve as repositories for regulatory information that influence every aspect of mRNA function. The 5' UTR is a key determinant of translational efficiency.<sup>62</sup> Secondary structures present in the 5' UTR can inhibit ribosome scanning preventing efficient formation of the preinitiation complex.<sup>4,47</sup>

A subset of mRNAs contain upstream open reading frames (uORFs) in their 5' UTRs.<sup>36</sup> Translation of uORFs generally comes at the expense of the main reading frame, although reinitiation has been observed.<sup>2,5,29,83</sup> Utilization of uORFs influences translation of oncogenic mRNAs and immune genes.<sup>71,74,82</sup> Far less is known regarding the role of uORFs in neuronal plasticity.

Inflammatory mediators that promote pain can also influence translation.<sup>57</sup> For example, nerve growth factor (NGF) activates the mammalian target of rapamycin (mTOR) kinase in nociceptors. Because mTOR indirectly controls the availability of the cap-binding protein eIF4E, NGF increases translation specifically at the step of initiation.<sup>33</sup> Cytokines such as interleukin 6 (IL-6) promote nociceptor sensitization through the mitogen-activated protein kinase (MAPK) pathway.<sup>56</sup> Interleukin 6 stimulates MAP kinase-interacting kinases (MNK1/2) that in turn phosphorylate eIF4E at a single site (serine 209).<sup>59</sup> Pharmacologic reduction or genetic elimination of eIF4E phosphorylation yields insensitivity to pain-associated behaviors caused by NGF or IL-6.<sup>59</sup> Thus, NGF and IL-6 collectively shape nascent protein synthesis through distinct mechanisms that converge on eIF4E.<sup>56</sup> It is unclear if nascent translation in noncoding transcripts or regions of mRNA is impacted by inflammatory mediators that cause nociceptor sensitization.

Signaling peptides are prominent in pain and are meticulously controlled. Particularly relevant to this work is the calcitonin gene-related peptide (CGRP). Alternative splicing of the *Calca* gene gives rise to processed mRNAs encoding either calcitonin in the thyroid or the CGRP in the nervous system.<sup>1,63</sup> Calcitonin gene-related peptide is among the

Sponsorships or competing interests that may be relevant to content are disclosed at the end of this article.

P. Barragan-Iglesias, N. Kunder, and A. Wangzhou contributed equally.

Data and code Availability: This article includes all data sets/code generated or analyzed during this study. Sequencing data have been deposited to GEO <https://www.ncbi.nlm.nih.gov/geo/query/acc.cgi?acc=GSE117043>.

<sup>a</sup> University of Texas at Dallas, School of Behavioral and Brain Sciences, Richardson, TX, United States, <sup>b</sup> Department of Physiology and Pharmacology, Center for Basic Sciences, Autonomous University of Aguascalientes, Aguascalientes, Mexico, <sup>c</sup> Department of Biological Sciences, University of Texas at Dallas, Richardson, TX, United States, <sup>d</sup> Department of Bioengineering, University of Texas at Dallas, Richardson, TX, United States, <sup>e</sup> Center for Advanced Pain Studies, University of Texas at Dallas, Richardson, TX, United States

\*Corresponding author. Address: Department of Biological Sciences, 800 W. Campbell Rd, RL10 BSB 12.510, Richardson, TX 75080. Tel.: 972-883-4186. E-mail address: Zachary.Campbell@utdallas.edu (Z.T. Campbell).

Supplemental digital content is available for this article. Direct URL citations appear in the printed text and are provided in the HTML and PDF versions of this article on the journal's Web site ([www.painjournalonline.com](http://www.painjournalonline.com)).

PAIN 162 (2021) 1864–1875

© 2021 International Association for the Study of Pain

<http://dx.doi.org/10.1097/j.pain.0000000000002191>

most intensely studied peptide neurotransmitters. Calcitonin gene-related peptide is predominantly located in A $\delta$  and C-afferent fibers and is exocytosed in response to noxious stimuli.<sup>24,25,32,49,65</sup> In addition to its role in the somatosensory system, CGRP is a potent vasodilator.<sup>11,65</sup> Calcitonin gene-related peptide receptors are Gs-protein coupled and are located primarily in the central nervous system, vasculature, and macrophages.<sup>6,65</sup> Anti-CGRP antibodies have emerged as therapeutics for migraine.<sup>79</sup> This underscores the importance of CGRP as a nociceptive mediator.

We previously applied ribosome profiling<sup>39</sup> to dorsal root ganglion (DRG) neurons isolated from adult mice.<sup>8</sup> Here, we comprehensively identify dynamic sites of translation in noncoding RNAs and regulatory regions of mRNA. We find a unique set of uORFs that are differentially used in cultured DRG neurons. We focus on a single uORF encoded by *Calca*. The uORF is repressive with respect to a downstream coding sequence (CDS). The uORF is translated in the context of the endogenous 5' sequence context when fused to a luciferase gene. We find that a novel peptide corresponding to the CGRP uORF promotes mechanical hypersensitivity and sensitization of nociceptors. Intriguingly, inhibition G $\alpha$ -q signaling blocks the nociceptive action of CUP. This suggests that the relevant but unknown receptor is a GPCR. Collectively, these findings uncover a role for uORF translation in nociceptor plasticity and suggest novel targets for the disruption of pain signaling in the periphery.

## 2. Methods

### 2.1. Experimental model and subject details

In vitro (ribosome profiling and reporter assays) and behavioral experiments were performed using wild-type male Swiss Webster mice (4-6 and 8-12 weeks old, respectively) purchased from Taconic laboratories. Moreover, multielectrode array (MEA) recording experiments were performed using 4- to 6-week-old ICR/CD1 mice. Animals were housed with a 12 hours light/dark cycle and had food and water available ad libitum. All animal procedures were approved by Institutional Animal Care and Use Committee at the University of Texas at Dallas and were in accordance with the International Association for the Study of Pain guidelines.

### 2.2. Ribosome profiling cultures, library generation, and sequencing

The library generation and sequencing were previously performed.<sup>8</sup> Dorsal root ganglia (C1-L5) were excised from 10 Swiss Webster mice per replicate and placed in chilled Hanks' balanced salt solution (HBSS; Invitrogen, Waltham, MA). After dissection, DRG were enzymatically dissociated with collagenase A (1 mg/mL, Roche, Basel, Switzerland) for 25 minutes and collagenase D (1 mg/mL, Roche) with papain (30 U/mL, Roche) for 20 min at 37°C. Dorsal root ganglia were then triturated in a 1:1 mixture of 1 mg/mL of trypsin inhibitor (Roche) and bovine serum albumin (BioPharm Laboratories, Bluffdale, UT), then filtered through a 70  $\mu$ m cell strainer (Corning). Cells were pelleted, then resuspended in DRG culture media: DMEM/F12 with GlutaMAX (Thermo Fisher Scientific, Waltham, MA) containing 10% fetal bovine serum (FBS; Thermo Fisher Scientific), 1% penicillin and

streptomycin, 5 ng/mL of NGF, and 3  $\mu$ g/mL of 5-fluorouridine with 7  $\mu$ g/mL of uridine to inhibit mitosis of nonneuronal cells. Cells were evenly distributed in 3 poly-D-lysine-coated culture dishes (100 mm diameter) (BD Falcon, Bedford, MA) and incubated at 37°C in a humidified 95% air/5% CO<sub>2</sub> incubator. DRG culture media was changed every other day, and cells were treated with NGF (20 ng/mL) and IL-6 (50 ng/mL) at day 6 for 20 minutes, followed by addition of emetine (50  $\mu$ g/mL) for 1 minute to protect the ribosome footprints.

### 2.3. Library generation and sequencing

Library generation and sequencing Libraries consisting of ribosome bound RNA fragments were generated as described with minor adjustments in the composition of the polysome lysis buffer (20 mM Tris-HCl, pH 7.5, 250 mM NaCl, 15 mM MgCl<sub>2</sub>, 1 mM DTT, 0.5% (vol/vol) Triton X-100, 2.5 U/mL DNase I, 40 U/mL RNasin, and 50  $\mu$ g/mL emetine).<sup>37,39</sup> MicroSpin S-400 columns (GE Healthcare, Chicago, IL) were used to isolate ribosome bound RNAs. After rRNA was removed using the RiboCop rRNA depletion kit (Lexogen, Vienna, Austria), footprints were dephosphorylated then size selected (28-34 nt) by PAGE on 15% TBE-Urea gels (Bio-Rad, Hercules, CA). Footprints were generated by SMARTer smRNA-Seq kit for Illumina (TaKaRa). RNA abundance was quantified using the QuantSeq 3' mRNA-Seq library kit (Lexogen). The concentrations of purified libraries were quantified using Qubit (Invitrogen), and the average size was determined by a fragment analyzer with high sensitivity NGS fragment analysis kit (Advanced Analytical Technologies Inc, Orangeburg, NY). Libraries were then sequenced on an Illumina NextSeq 500 sequencer using 75-bp single-end high output reagents (Illumina). After sequencing, files were downloaded from a BaseSpace onsite server. An Initial quality check was conducted using FastQC 0.11.5 (Babraham Bioinformatics, Cambridge, United Kingdom). Adapters were subject to trimming based on adapter sequences. Mapping was conducted with TopHat 2.1.1 (with Bowtie 2.2.9) to the mouse reference genome (NCBI reference assembly GRCm38.p4) and reference transcriptome (Gencode vM10). Strand orientation was considered during the mapping process. Processed bam files were quantified for each gene using Cufflinks 2.2.1 with gencode.vM10 genome annotation. Read counts were not normalized by length by using the Cufflinks option—no-length-correction. Relative abundance for the *i*th gene was determined by calculating transcripts per million (TPM) values as follows:

$$\text{TPM}_i = 10^6 \times \frac{a_i}{\sum_j [a_j]}$$

where  $a_i$  is the Cufflinks reported relative abundance. Finally, TPM values were normalized to upper decile for each biological replicate, and upper decile TPM (udTPM) values were used for analysis,<sup>34</sup> to provide uniform processing for samples with varying sequencing depth.

#### 2.4. Fragment length organization similarity scores

All of the samples from either the control group (4 replicates) or plasticity treatment group (4 replicates) were pooled to increase sequencing depth (GEO accession number: GSE117043). Fragment length organization similarity scores (FLOSSs) were calculated according to the following equation defined by<sup>40</sup>:

$$\text{FLOSS} = \frac{\sum_{\text{read length}} |\text{Distribution}_{1_{\text{read length}}} - \text{Distribution}_{2_{\text{read length}}}|}{2}$$

where  $\text{Distribution}_{1_{\text{read length}}}$  refers to the FLOSS distribution for a given region or transcript class.  $\text{Distribution}_{2_{\text{read length}}}$  is the distribution of the CDS regions in aggregate and serves as the reference sample for coding potential. The cutoff for the CDS FLOSS was interpolated from the 95th percentile of the FLOSSs (using a slotted window between 0 and 3.9 with increments of 0.3).

#### 2.5. Upstream open reading frame detection

To define uORFs, the gencode mouse genome mm10 (GRCm38) was scanned for the standard (ATG) and degenerate start codons (NTG) with in frame stop codons 4 to 50 amino acids downstream. Three criteria were used to filter uORFs. First, the sum of the base-wise coverage (SBWC) for a given uORF had to exceed 0.01% of the total mapped reads in the corresponding condition. Second, to account for uniformity of the read distribution at the initiation site, the base-wise coverage for the first 15 bp of the uORF was constrained to be between 50% and 150% of the average base-wise coverage of these 15 bp. Finally, because ribosomes accumulate at the 5' end of bona fide initiation sites, the SBWC within 15 bp of the initiation site was constrained to a minimum of 33% of the SBWC of the uORF.

#### 2.6. Reporter assays

The *Calca* 5' UTR was cloned upstream of a firefly luciferase gene using Gibson assembly in a PGL4.13 vector (Promega, Madison, WI).<sup>31</sup> Site-directed mutagenesis was used to generate uORF mutants that lacked coding potential with the following primer set (5' accgcttcgaagcaccctggctccatcaggatc and 5' gatcctgatgagccagggggtgcttgcgaagcggt).

The entire uORF sequence with a CTG/TGA start codon and a mutated stop codon (GGG) was fused to a firefly luciferase gene having a mutated start codon (GGG). The entire insert was Gibson cloned into a pCDNA3—9XMyc vector. Before electroporation, DRG from the C1-L5 spinal segment were excised aseptically and placed in chilled HBSS (Invitrogen). Dorsal root ganglia were enzymatically digested and triturated as described above. Cells were then pelleted through centrifugation, counted on a hemocytometer using trypan blue, and then resuspended in DRG culture media. The P3—Primary Cell 4D—Nucleofector X Kit (Lonza) was used to nucleofect the firefly luciferase and renilla luciferase constructs into DRG neurons per manufacturer's instructions. The nucleofected cells were then plated on to a poly-D-lysine-coated 96-well plate in DRG culture media. Cultures were incubated at 37°C in a humidified 95% air/5% CO<sub>2</sub> incubator for 2 days. The Dual-Luciferase Reporter 1000 Assay Systems (Promega) was used to assay luciferase activity on a luminometer (Turner Biosystems). The

media was then removed, and cells were washed with 1X PBS to remove residual media. To each well, 60 μL of 1X passive lysis buffer was added and incubated at room temperature for 15 minutes on a shaker. To 20 μL of cell lysate, 50 μL of LAR II was mixed and luminescence for the firefly luciferase (fluc) was measured. Samples were vortexed and 50 μL of Stop & Glo Reagent was used to determine *Renilla* luciferase (rluc) activity.

#### 2.7. Dorsal root ganglion dissociation and multielectrode array culture seeding

Dorsal root ganglia were collected from 4- to 6-week-old ICR/CD1 mice. Young ICR/CD1 mice cultures produce detectable spontaneous and evoked extracellular spikes using a 12-well recording plate (Axion Biosystems, Atlanta, GA) over a time course of 3 to 13 days after plating.<sup>13</sup> Dorsal root ganglia were placed in enzymatic dissociation solution containing 2 mg/mL of collagenase in HBSS. Dorsal root ganglia were incubated for 45 minutes at 37°C. Dissociation solution was then supplemented with 0.025% trypsin for 5 to 10 additional minutes at 37°C. The remaining tissue was mechanically triturated using a fire-polished Pasteur pipette until solution appeared homogeneous. Dissociated cell solution was passed through a 70 μm sieve and then centrifuged at 300×g for 5 minutes to purify and collect sensory neurons. Neurons were seeded on 12-well MEA plates (Axion Biosystems), which had been previously treated with 0.1% PEI and 20 μg/mL laminin at 10,000 neurons/well. Wells were subsequently flooded with 600 μL of culture medium, as described in the ribosome profiling culture section, supplemented with 5 ng/mL GDNF. Dorsal root ganglion-MEA cultures were maintained in cell culture incubators at 37°C, 10% CO<sub>2</sub>, and 95% humidity.

#### 2.8. Multielectrode array recordings and analysis

Spontaneous and evoked extracellular recordings were performed using an Axion Maestro recording system and 12-well recording plates (Axion Biosystems) as previously described.<sup>13</sup> Briefly, filtered continuous recordings were collected from all 12 wells (768 total electrodes) simultaneously at 12.5 kHz sampling rate. Extracellular spikes were defined as filtered continuous data crossing an adaptive threshold of  $\pm 5.5\sigma$  based on 1-second snapshots of root mean squared noise. Active electrodes were defined as those exhibiting a minimum of 1 spike/min during baseline spontaneous extracellular recordings and were used in further analyses. Spontaneous neuronal activity was recorded every alternate day beginning day-in-vitro (DIV) 3 to confirm viable culture conditions and to detect stable spontaneous baselines similar to those previously reported.<sup>13,59</sup> Upstream open reading frame experiments were conducted between DIV 11 and 13 on cultures exhibiting at least 4 spontaneously active electrodes per well. Environmental conditions (37°C, 10% CO<sub>2</sub>, and 95% humidity) were maintained throughout the recording duration unless otherwise noted (ie, during temperature-evoked activity recordings).

For each uORF concentration, experiments consisted of 4 periods. (1) After baseline recordings, (2) Scramble or CGRP uORF peptide (henceforth referred to as CUP) was added to previously active wells, and all cultures were replaced in the cell culture incubator for 2.5 hours. (3) Cultures were removed from the cell



incubator, placed in the Axion recording system, and allowed to acclimate for 30 minutes. Spontaneous activity was then recorded for 15 minutes. (4) Immediately after the spontaneous activity recording, temperature responsiveness was evaluated by subjecting cultures to a temperature increase (37–42°C) through Axion's base plate temperature control. Temperature-responsive electrodes were defined as electrodes that exhibited a minimum of 2-fold increase in activity during the heating period as compared to baseline activity. This process was immediately repeated for 10 and 100 nM concentrations using the same cultures. This process was subsequently repeated for CUP (100 nM) in the presence of YM-254890 (100 nM). The median spontaneous firing rates were calculated for each well, excluding inactive electrodes. Fold change in the median firing rate was calculated as the ratio of spontaneous activity at each treatment concentration to initial, untreated spontaneous activity. In the case of CUP vs Scramble treatments, outcomes were compared across concentrations using a two-way analysis of variance, followed by a two-sample *t* test, with  $P < 0.05$  indicating statistical significance. Using a two-sample *t* test, 100 nM concentrations, including YM-254890, were also compared pairwise. Treatments were compared at each concentration using a two-sample test of proportions, with  $P < 0.05$  indicating statistical significance.

### 2.9. Thermal and mechanical behavioral testing

Mice were randomized to groups from multiple cages to avoid using mice from experimental groups that were cohabitating. At the time of the testing, 2 experimenters were blinded to the experimental conditions. To measure the mechanical sensitivity, mice were placed in acrylic boxes with wire mesh floors, and baseline plantar mechanical sensitivity was measured after habituation for 1 h using the up-down method.<sup>17</sup> Briefly, calibrated von Frey filaments (Stoelting, Wood Dale, IL) were applied to the plantar surface of the hind paw for 1 to 3 seconds, and the up-down method was used to estimate the withdrawal mechanical threshold in grams (g). To measure thermal sensitivity, we used the Hargreaves test to determine the paw withdrawal latency in a separate group of mice.<sup>35</sup> Mice were placed on a glass floor and a focused beam of high-intensity light was aimed at the plantar surface of the hind paw. The light intensity was set to 40% following manufacturer's instructions (IITC Model 390) with a cutoff value of 20 seconds. To decrease the experimental variability between groups, the hind paw withdrawal latency was measured in triplicate with each trial being separated by at least 10 minutes. After determining baseline withdrawal thresholds, we sought to characterize the nociceptive actions of the uORF-encoded peptides, we tested mechanical and thermal sensitivity at various time points after intraplantar hind paw administration of either Scramble or CUP (GL Biochem) at 3 µg. The dose of CUP was chosen based on previous pilot studies where we found that nanogram doses do not produce a statistically significant increase in mechanical or thermal pain responses in mice when injected intraplantarly.

When animals returned to their original baseline thresholds at day 9, priming was revealed by an intraplantar injection of PGE<sub>2</sub>, and the mechanical hypersensitivity was again assessed at 24 hours after PGE<sub>2</sub> administration.

### 2.10. Statistical analysis

Behavioral testing data are shown as means ± SEM of at least 6 animals per group. For behavior experiments, the sample size was estimated as  $n = 6$  using G\*power for a power calculation with 80% power, expectations of 50% effect size, with  $\alpha$  set to 0.05. Graph

plotting and statistical analysis used GraphPad Prism version 7.0 (GraphPad software). The Student *t* test was used to compare 2 independent groups. Statistical evaluation for 3 independent groups or more was performed by one-way or two-way analysis of variance, followed by post hoc Bonferroni, and the a priori level of significance at 95% confidence level was considered at  $P < 0.05$ . Specific statistical tests used are described in figure legends. The significance of gene expression level changes before and after the treatment was calculated using a 2-tailed Student *t* test assuming unequal variances.

## 3. Results

### 3.1. Noncanonical sites of translation are used in dorsal root ganglion neurons

We previously conducted ribosome profiling on cultured DRG neurons subjected to either a vehicle or a plasticity treatment consisting of a combination of NGF and IL-6.<sup>8</sup> Here, we focus on translation in noncoding and untranslated regions of mRNA. To identify bona fide sites of translation, we set out to discriminate true ribosome footprints from contaminants. Ribosomes arrested during translation possess a characteristic footprint length.<sup>41</sup> Fragment length organization similarity score provides a quantitative means to compare distributions of ribosome-protected footprint sizes for a transcript vs an ideal footprint distribution derived from the mRNA coding region (Figs. 1A–C).<sup>40</sup> Coding regions yield a normal distribution centered on an average of 30 base pairs in the presence of emetine. The more closely a transcript or class of transcript resembles the ideal distribution, the FLOSS value will approach zero. The accuracy of FLOSS measurements is related to the number of reads for a given gene (Fig. 1D). For CDS regions with many reads, FLOSSs for coding regions approach zero, whereas genes with CDS regions with few reads show a broad distribution of FLOSSs. The FLOSS cutoff (Fig. 1D) indicates coding potential based on mRNA CDS values. To calculate the curve, a sliding window for each read count was used to determine outlier values. We consider transcripts below the curve as having passed the FLOSS threshold for exclusion. We examined FLOSSs for the following: noncoding (0.18 vehicle, 0.12 treated, Figs. 1A and B), long noncoding (0.27 vehicle, 0.16 treated), and mitochondrial mRNAs (0.27 vehicle, 0.28 treated). Unlike noncoding and mitochondrial transcripts, long noncoding RNAs (lncRNAs) displayed large changes in aggregate FLOSS after plasticity treatment (Figs. 1B and C).

The fidelity of translation termination is subject to dynamic control.<sup>22</sup> Decoding of the stop codon is essential for numerous processes such as incorporation of amino acid recoding of selenocysteine,<sup>67</sup> viral replication,<sup>10,27,46</sup> suppression of pathological consequences of deleterious phenotypes caused by premature termination codons, and extension of the carboxy-terminus. Readthrough is a conserved process across humans, yeast, and *Drosophila* but is not well characterized in mice.<sup>23</sup> Bypass of the stop codon can change key aspects of protein function such as changes in subcellular localization and protein aggregation.<sup>23</sup> Indeed, drugs that promote readthrough of premature termination codons such as gentamicin also cause cellular toxicity.<sup>38,52</sup> In the mouse DRG, we observe many instances of ribosome occupancy in the 3' UTR (FLOSS = 0.34 vehicle and 0.26 treated, Figs. S1A–C, available at <http://links.lww.com/PAIN/B258>). Ribosome footprints are prominent after the stop codons of *Rps28* and *Eif4a2* and are sensitive to the plasticity treatment (Figs. S1D–E, available at <http://links.lww.com/PAIN/B258>).<sup>42</sup> Readthrough of the termination codon in *Rps28* has also been reported in human fibroblasts suggestive of broad conservation across mammals.<sup>23</sup>

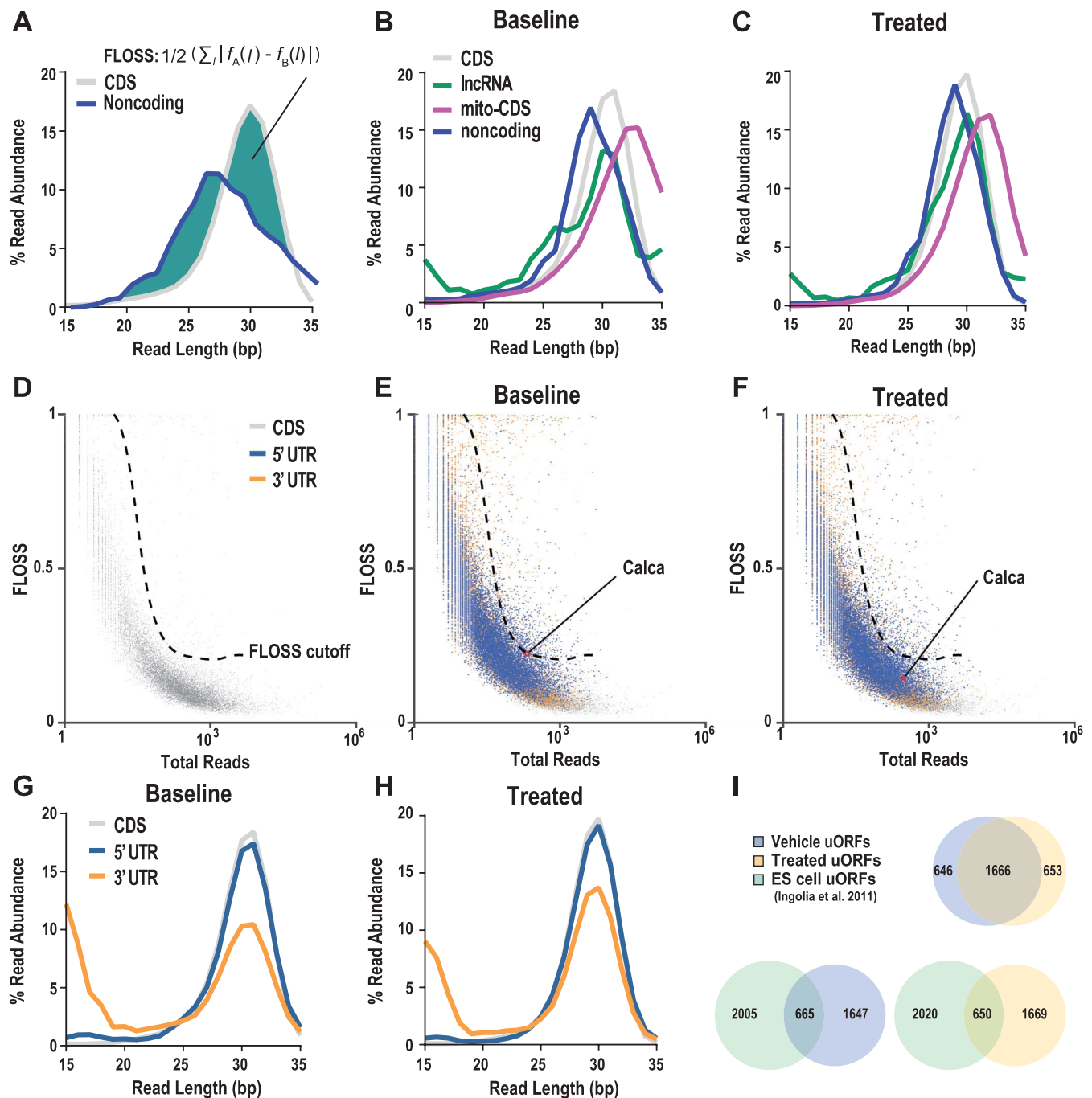


**Figure 1.** Ribosome profiling identifies uORFs in 5' untranslated regions of mRNA in cultured DRG neurons. (A) A schematic illustrates the calculation of FLOSS values based on the discrepancy (solid green) between a transcript, region of a transcript, or transcript class (noncoding RNA blue) vs the coding region of mRNA (grey). The FLOSS equation is provided. (B and C) Read length distributions for transcript sequences of CDS (grey), lncRNAs (green), mitochondrial mRNAs (magenta), and noncoding RNAs (blue) after vehicle or plasticity treatments. (D–F) FLOSS distributions for coding regions (grey) of all protein-coding gene mRNAs overlaid with 5' (blue) and 3' (orange) UTRs under baseline conditions (E) or after addition of the plasticity treatment (F). The 5' UTR of *Calca* is highlighted in (E) and (F). The FLOSS cutoff is indicated as a dashed line and indicates regions of the plot with a high potential for being coded. (G and H) Read length distribution for protein coding sequence (grey), 5' UTR (blue), and 3' UTR (orange) after an exposure to vehicle or after plasticity treatment, respectively. (I) Venn diagrams depict the number of uORFs detected in DRG cultures treated with vehicle or plasticity treatment vs those found in mouse embryonic stem cells.<sup>42</sup> CDS, downstream coding sequence; DRG, dorsal root ganglion; FLOSS, fragment length organization similarity score; uORF, upstream open reading frame; UTR, untranslated region.

### 3.2. A upstream open reading frame-encoded peptide that is linked to pain

We observed pervasive ribosome occupancy in 5' UTRs (FLOSS = 0.05 vehicle and 0.03 treated, **Figs. 1D–H**). FLOSS values for many 5'UTRs are similar to those of CDS regions. Yet, when FLOSS scores are...are aggregated for all genes, 5' UTRs

undergo a small shift that increases their similarity to CDS (**Figs. 1E–H, S2A–D**). Many of these events seem to be tissue specific because only 30% of uORFs detected in the DRG are also used in mouse embryonic stem cells (Fig. 1I, Supplemental Table 1, available at <http://links.lww.com/PAIN/B259>).<sup>42</sup> We found that the FLOSS value of the *Calca* 5' UTR are beneath the FLOSS cutoff indicative of

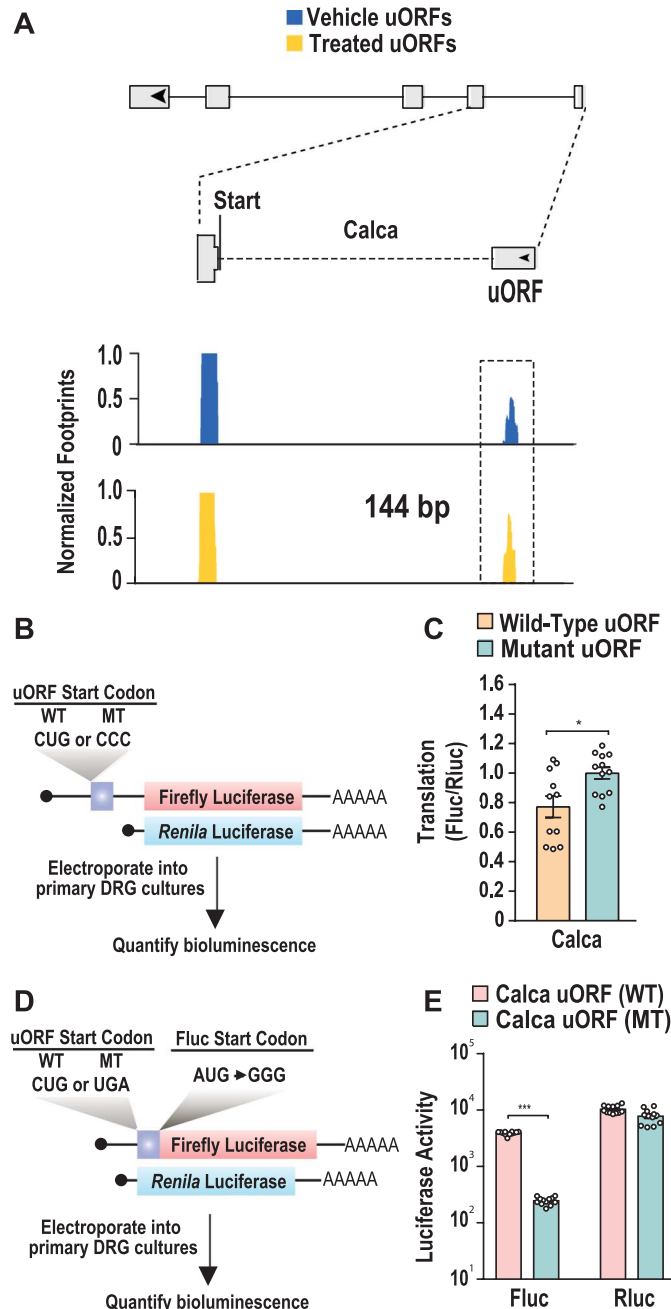


**Figure 2.** Translation in untranslated regions occurs on transcripts linked to pain. (A) Ribosome-protected footprints situated in the 5' UTR of *Calca*. (B) A schematic of dual-luciferase reporters for the translational modulation of downstream coding regions by the *Calca* uORF. The *Calca* 5' UTR was cloned upstream of a firefly luciferase construct. Translation from the *Calca* uORF is discontinuous to that from the downstream luciferase ORF. Vectors were electroporated into primary DRG cultures before the quantification of reporter gene activity. (C) Dual-luciferase assays for the *Calca* uORF. The *Calca* uORF represses downstream translation of the main ORF by 20%. This repression is eliminated through mutation of the *Calca* uORF start codon (CUG) to (CCC). Data are plotted as mean  $\pm$  SEM. The Student unpaired *t* test: CGRP wild-type uORF vs mutant uORF:  $*P = 0.0135$ ,  $n = 12$  cultures. (D) Detection of uORF translation through the use of a translational fusion to a luciferase reporter. The *Calca* uORF was cloned in a frame with luciferase. To eliminate the utilization of the start codon (ATG) of the luciferase reporter, it was mutated to GGG. Vectors were electroporated into primary DRG cultures before luciferase quantification. (E) Dual-luciferase assays for uORF translation. Luciferase activity is observed in the presence of the uORF start codon (CUG) indicating translation of the *Calca* uORF. Luciferase activity was abolished on mutating the start codon (CUG) to stop codon (UGA).  $n = 12$  cultures. Data are plotted as mean  $\pm$  SEM. The Student unpaired *t* test: *Calca* wild-type leader vs mutant leader sequence:  $*P = 0.00,001$ . CGRP, calcitonin gene-related peptide; DRG, dorsal root ganglion; uORF, upstream open reading frame; UTR, untranslated region.

a high probability of ribosome occupancy (Figs. 2A–B, available at <http://links.lww.com/PAIN/B258>). Mutations in *Calca* are linked to visceral, neuropathic, headache, and inflammatory pain.<sup>3,28,45,73</sup> The FLOSS values for the *Calca* 5' UTR overlap with those corresponding to coding transcripts with similar read counts (Figs. 1E–F). This led us to ask if the *Calca* 5' UTR encodes a uORF.

To probe the *Calca* uORF, a series of chimeric luciferase constructs were generated and introduced into primary DRG neurons by nucleofection (Fig. 2C). The *Calca* 5' UTR was cloned upstream of a firefly reporter construct. In the reporter and the endogenous context, the translation of the uORF is discontinuous from the primary ORF. The reporter constructs encoded either

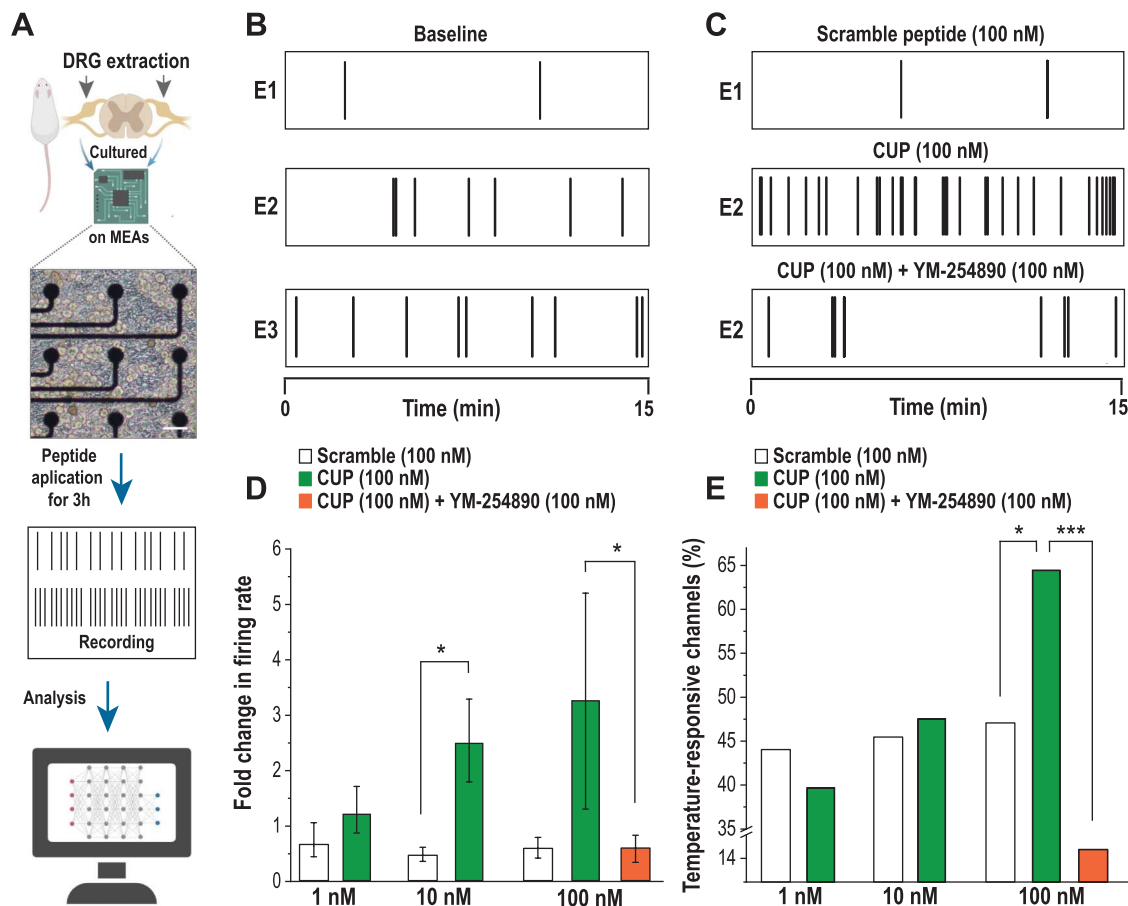


**Figure 3.** CUP promotes sensory neuron excitability. (A) A schematic of the multi-electrode array system. White scale bar corresponds to 50  $\mu\text{m}$ . (B) Baseline recordings of spontaneous activity for 3 individual electrodes. (C) Activities after addition of 100 nM of Scramble (E1) peptide, CUP (E2), or the combination of CUP in the presence of YM-254890 (E3) after a three-hour incubation. (D) CUP (1–100 nM) peptide led to increased spontaneous firing rates after a three-hour incubation. A spontaneous firing rate is attenuated in the presence of the Gq inhibitor YM-254890. Two-way ANOVA:  $F_{(2, 4)} = 3.48$ ,  $P = 0.03$ . The Bonferroni test. \* $P = 0.032$ . Scramble vs CUP at 10 nM: # $P = 0.031$ . CUP vs CUP + YM-254890 at 100 nM: \* $P = 0.045$ . (E) CUP (100 nM) increased the percentage of temperature-responsive MEA channels. The percentage of temperature-responsive MEA channels is decreased in the presence of YM-254890. The two-sample test of proportions. Scramble vs CUP at 100 nM: \* $P = 0.026$ . CUP vs CUP + YM-254890 at 100 nM: \*\*\* $P < 0.001$ . ANOVA, analysis of variance; CUP, CGRP uORF peptide; MEA, multi-electrode array.

the wild-type uORF start codon (CUG) or a mutant (CCC). A second luciferase vector encoding *Renilla* luciferase was used as an internal control. To test for translation of each uORF, we assayed the ratio of the 2 reporters with or without start sites. We found that the uORF results in approximately 20% repression of the downstream reading frame (Fig. 2D). An effect size of 20% is consistent with previous studies on uORF repression.<sup>16,19,44,72</sup> This effect was dependent on the presence of a near-cognate start site (CUG) as mutations to that eliminate coding potential (CCC) abrogated repression. To test if the uORF is translated, the *Calca* uORF was cloned in a frame with a firefly luciferase reporter (Fig. 2E). To ensure that the start codon of the firefly reporter was not used, it was mutated to GGG. In this series of assays, translation of the uORF with its natural start site (CUG) was compared with mutants with a stop codon (UGA) mutation in place of the start site. We find that translation driven by the *Calca* uORF is robust and requires a near-cognate start site (Fig. 2F).

### 3.3. A pronociceptive peptide encoded by the *Calca* upstream open reading frame

Because the 5' UTR has emerged as a potential source of functional peptides,<sup>74</sup> we asked if the CUP peptide encoded by

*Calca* is biologically active. Extracellular recordings of DRG neurons were collected using MEAs (Figs. 3A–C). Peptides (CUP: LPGSIRIPAGSAPRHRSPGEP or Scramble: RISLPGPSGIARAPRSHEPPG) were incubated for 3 hours before recording. Addition of 10 and 100 nM CUP enhanced spontaneous firing rates (Fig. 3D). Importantly, the scrambled peptide had no effect. Furthermore, at 100 nM concentration, CUP sensitized nociceptors to thermal stimulation in the noxious range (Fig. 3E). The scrambled peptide again had no effect. Given that many neuroactive peptides increase nociceptor excitability by acting on GPCRs that stimulate Gq, we hypothesized that the uORF-encoded peptide might also function through Gq-mediated GPCR signaling. Therefore, we examined if nociceptors were sensitized by CUP (100 nM) in the presence of the Gq inhibitor YM-254890 (100 nM). We found that spontaneous firing was reduced to baseline levels and temperature responsiveness was similarly decreased (Figs. 3D–E). These data indicate that CUP-induced neuronal hyperexcitability is mechanistically linked to a Gq-signaling pathway.

To characterize the potential role of CUP in vivo, we evaluated mechanical allodynia using von Frey filaments. We injected either CUP or a scramble peptide into the hind paw of mice and assayed mechanical sensitivity (Fig. 4). We found

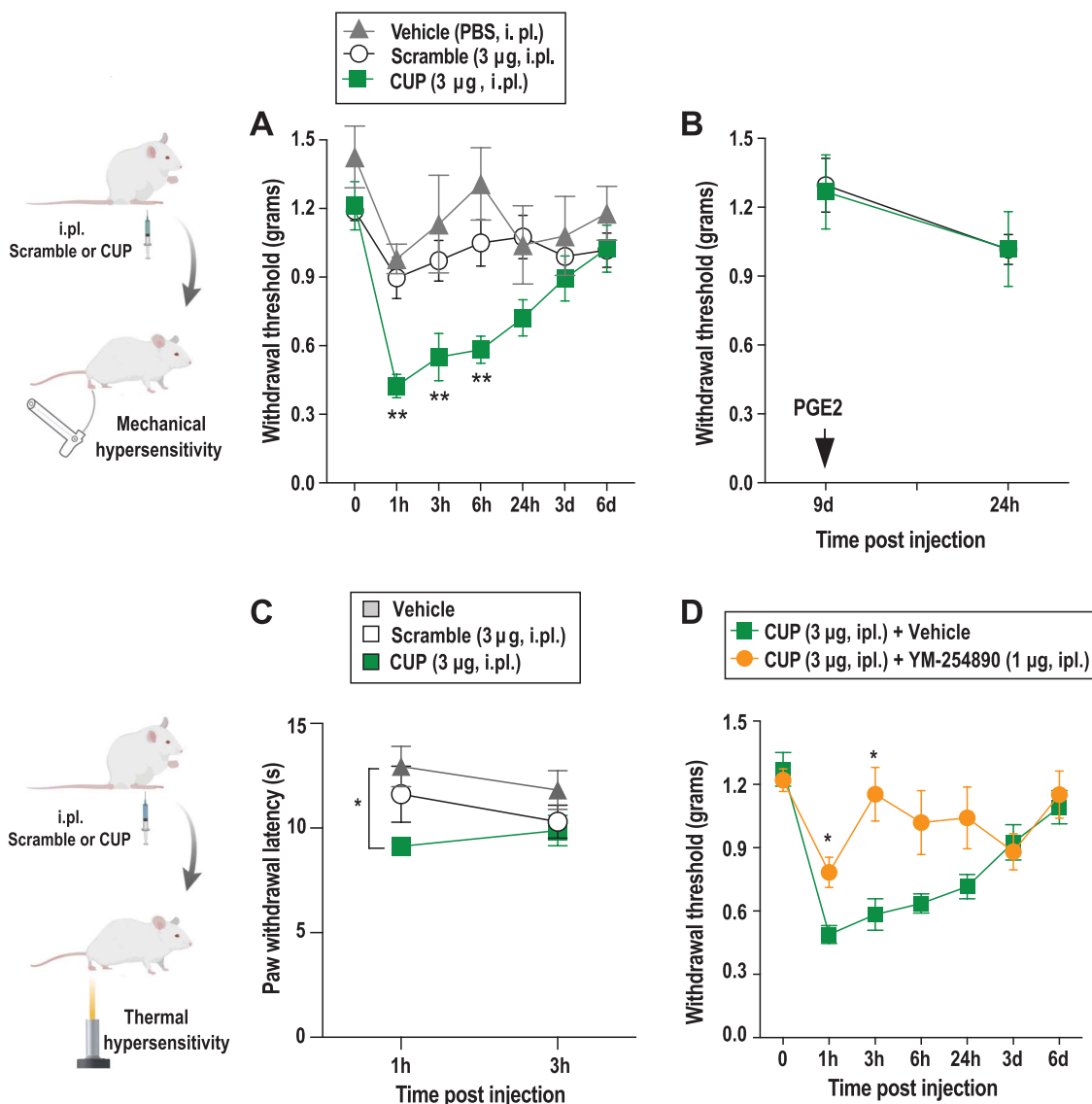


**Figure 4.** CUP induces pronociceptive responses to mechanical and thermal stimulation. (A) Intraplantar administration of CUP at 3 μg, but not scrambled peptide at the same dose, induces mechanical hypersensitivity. Two-way repeated measures (RM) ANOVA:  $F_{(1, 22)} = 13.56, P = 0.0013$ . The Bonferroni multiple comparison test. Scramble vs CUP at 1 hour:  $**P = 0.0018$ , at 3 hours:  $*P = 0.0370$ , at 6 hours:  $**P = 0.0062$ . (B) Intraplantar administration of CUP (3 μg) did not induce changes in mechanical sensitivity at day 9 after the injection of prostaglandin E2 (PGE2, 100 ng, i.pl.). (C) Changes in pain sensitivity to thermal stimulation are detected after i.pl. scramble or CUP administration. Two-way RM ANOVA with RM:  $F_{(1, 11)} = 6.30, P = 0.0215$ . The Bonferroni multiple comparisons test: vehicle vs CUP at 1 hour:  $*P = 0.0467$ . (D) Intraplantar administration of YM-254890 (a Gq inhibitor; 1 g) attenuates CUP-induced mechanical hypersensitivity. Two-way RM ANOVA:  $F_{(1, 22)} = 6.130, P = 0.0215$ . The Bonferroni multiple comparisons test. CUP vs CUP + YM-254890 at 1 hour:  $*P = 0.0467$ ; at 3 hours:  $*P = 0.0280$ . ANOVA, analysis of variance; CUP, CGRP uORF peptide.

that intraplantar administration of CUP, but not the scrambled peptide, produced mechanical hypersensitivity that lasted for at least 6 hours (Fig. 4A). However, there was no effect on mechanical withdrawal thresholds when the animals were subsequently challenged with a subthreshold dose of PGE2 (Fig. 4B). Hyperalgesic priming refers to a model where the initial sensitization is allowed to resolve after which point a second subthreshold stimulus is injected.<sup>61</sup> Stimuli promote plasticity in the nociceptive system prime animals such that the second stimulus results in prolonged sensitivity to sensory inputs. This event is frequently associated with the process underlying the transition from acute to chronic pain.<sup>61</sup> Our results indicate that CUP promotes acute sensitization but does not induce hyperalgesic priming. CUP increased thermal sensitivity slightly 1 hour after injection; the difference between

vehicle-injected paws and those that received CUP was significant but not at the 3-hour time point (Fig. 4C). Finally, to probe how CUP functions in vivo, we again blocked Gq signaling. Injection of YM-254890 did not produce significant changes in mechanical hypersensitivity (Supplementary Fig. 3, available at <http://links.lww.com/PAIN/B258>). However, mechanical allodynia caused by CUP was attenuated by co-administration with YM-254890 (1 μg) (Fig. 4D). Taken together, these results suggest that a uORF-encoded peptide can promote rapid changes in nociceptor excitability (Fig. 5A). We favor the model that this is likely through GPCR signaling, resulting in pain-like behavioral responses to mechanical stimulation in vivo (Fig. 5B). In addition, we found modest differences in thermal responsiveness after the injection of



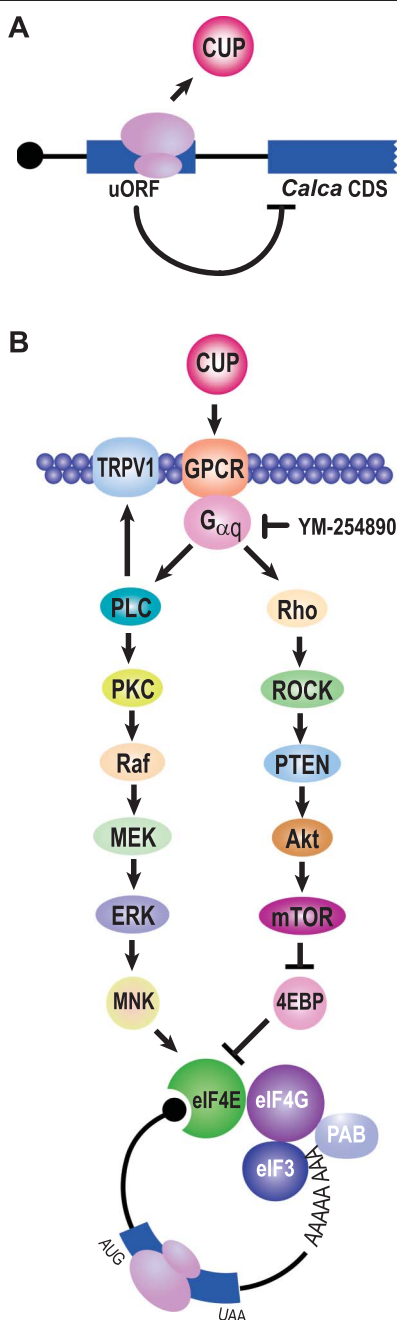


**Figure 5.** Schematic of *Calca* translation and potential mechanisms of nociceptive sensitization by CUP. (A) A uORF present in *Calca* results in the production of a peptide termed CUP. The utilization of the uORF represses the translation of the primary reading frame. (B) Potential mechanisms of sensitization by CUP. CUP sensitizes the nociceptive system through Gq signaling. First, the activation of Gq results in phosphorylation and sensitization of TRPV1.<sup>12</sup> Gq signaling promotes phospholipase C (PLC) activation.<sup>80</sup> Phospholipase C generates diacylglycerol (DAG) and inositol trisphosphate (IP<sub>3</sub>). A key consequence of these secondary messengers is the activation of protein kinase C (PKC). Protein kinase C stimulates multiple pathways including MAPK signaling.<sup>69</sup> Protein kinase C activates Raf that activates MEK, ERK, and ultimately MNK. MNK phosphorylates eIF4E and promotes nociception.<sup>59</sup> Conversely, Gq also stimulates the Rho kinase.<sup>20</sup> Rho activates the Rho-associated protein kinase (ROCK). ROCK activates PTEN, a key upstream regulatory component of PI3K/mTOR signaling.<sup>50</sup> PTEN controls Akt that ultimately stimulates mTOR. Mammalian target of rapamycin promotes cap-dependent translation through the negative regulation of 4EBPs that sequester eIF4E. CUP, CGRP uORF peptide; mTOR, mammalian target of rapamycin; MAPK, mitogen-activated protein kinase; uORF, upstream open reading frame.

CUP in vivo and sensitized thermal responses at higher concentrations in vitro (Fig. 5B).

#### 4. Discussion

Our data support 4 key findings. First, noncoding RNA is resplendent with potential sites of translation in DRG neurons. Second, the uORF utilization is broadly distinct in the DRG. Third, a newly identified uORF present in *Calca* encodes a peptide that promotes sensitization of nociceptors. Finally, sensitization by this peptide seems to involve Gq signaling. We discuss each finding in turn.

We describe the landscape of nascent translation in the DRG in response to a plasticity treatment. To the best of our knowledge, this work constitutes one of the first reports to use ribosome profiling in this context. A related experiment used this approach to profile translational landscapes as a function of spared nerve injury in the DRG and spinal cord.<sup>78</sup> This landmark report established the feasibility of tissue experiments and identified changes in translational efficiencies of mRNA that could be the result of activated ERK signaling. Parallel investigations used ribosome pull-down and mass spectrometry approaches to profile translation, adding to our understanding of translational control of mRNA.<sup>54,55,64</sup> The union of nociceptor-specific ribosome pull down with ribosome profiling could greatly improve the specificity of the approach and enable more precise measurements in vivo. Unlike related experiments in the brain, obtaining sufficient starting material remains a significant obstacle.<sup>37</sup>

Regulated protein biosynthesis is required for nociception; we propose that noncoding RNA regions may yield functionally relevant polypeptides.<sup>26,48,51</sup> We identified instances of ribosome occupancy in multiple classes of noncoding RNA. We have examined a single case where a noncoding region is translated to produce a signaling peptide. Yet, there are hundreds of uORFs that are distinct from embryonic stem cells.<sup>40</sup> Understanding their biological roles is crucial. Many uORFs and lncRNAs yield peptides that regulate proliferation in cell lines.<sup>18</sup> The role of uORF-encoded peptides in biology is continually expanding. For example, ribosome profiling in tumors revealed the presence of a functional uORF in programmed-death-ligand 1 (PD-L1).<sup>82</sup> The PD-L1 uORF is efficiently translated in cells. Mutation of the uORF increased PD-L1 abundance and metastatic potential in vivo. Although this work underscores the importance of a uORF in cancer, it does not elucidate a biological function of the peptide encoded by the uORF—a key focus of our work. The uORF-encoded peptides play prominent roles in immunity. Upstream ORF translation in the binding immunoglobulin protein (BiP) mRNA is initiated from a non-AUG codon.<sup>74</sup> Intriguingly, stress triggers presentation of uORF-encoded peptides through MHC-I. Although the dynamics of uORF translation have been investigated in the nervous system, our understanding of their biological functions remains tenuous.<sup>15,62</sup> This work elevates the importance of untranslated regions of mRNAs in nociception and extends the role of uORF translation into an in vivo context.

Injection of CUP triggered mechanical hypersensitivity. What is the cellular specificity of CUP? We favor DRG neurons as the targeted cell type because of the restricted pattern of expression of *Calca* and the definitive electrophysiological effects on these neurons in our experiments. An unambiguous means to determine where the peptide acts in vivo could involve direct visualization with immunohistochemistry. Our attempts to generate peptide antibodies have been unsuccessful, possibly

because of poor immunogenicity. In addition, we have examined mass spectrometry data, but because of the small size of tryptic peptides resulting from trypsin digests of CUP, the small size of the fragments (~700 Da or less) greatly complicates their detection. Although neurogenic inflammation is driven by CGRP release that acts on blood vessels, it remains unclear which cells are responsive to CUP. Given that sensitization occurred in culture conditions lacking blood vessels, and the limited survival of immune cells, our results are consistent with a neuronal mechanism but do not discount the possibility that CUP acts on other cell types as well.

Gq signaling has been implicated in nociception and is also required for sensitization mediated by the CUP peptide.<sup>77,81</sup> There are several potential mechanisms through which the CUP peptide might function (Fig. 5B). We provide 2 lines of evidence in support of the idea that Gq signaling is critical. First, the inhibition of Gq signaling with YM-254890 blocks sensitization by CUP in vivo and in vitro. Second, the modest, yet significant, effect on thermal sensitivity parallels numerous ligands, such as substance P, PGE<sub>2</sub>, PGI<sub>2</sub>, UTP, serotonin, and bradykinin, all of which use protein kinase C (PKC)/Gq signaling.<sup>7,9,53,58,60,66,68,70,75,76,84,85</sup> A relevant target of PKC signaling is the capsaicin and heat-responsive cation channel TRPV1. Activated Gαq/11-coupled receptors causes PLC to hydrolyze phosphatidylinositol 1,4, bisphosphate (PIP<sub>2</sub>) into inositol 1,4,5 trisphosphate (IP<sub>3</sub>) and diacylglycerol (DAG). PKC activity is stimulated by DAG and it directly stimulates TRPV1 through phosphorylation.<sup>9</sup> Injection of the CUP peptide resulted in a small increase in sensitivity to thermal stimuli at an early time point consistent with a mechanism of action that involves PKC. Although our data do not discount the involvement of additional pathways downstream of CUP, they add to the broad assortment of nociceptive mediators that require Gq signaling. CUP evoked more substantial changes in mechanical sensitivity than thermal in vivo. There are numerous pathways through which sensitization could occur. For example, activation of Rho would trigger increased mTOR signaling.<sup>30,43</sup> Alternatively, PLC/PKC signaling stimulates MAPK signaling.<sup>14,59</sup> Either mechanism could mediate biosynthesis of proteins that promote sensitization.

In conclusion, protein biosynthesis is key to the activity of nociceptors. The application of ribosome profiling to the DRG enables new opportunities to identify noncoding transcripts subject to dynamic changes in translation after the addition of a plasticity treatment. We find that a peptide encoded by a 5' UTR is sufficient to trigger sensitization and mechanical hypersensitivity in vivo. This result suggests a new repository for sequences that may encode neurotransmitters and opens the door to additional regulatory complexity. This is an important nuance that suggests additional regulatory complexity with a high degree of tissue specificity.

### Conflict of interest statement

The authors have no conflicts of interest to declare.

### Acknowledgements

This work was supported by NIH grants R01NS065926 (T.J.P.), R01NS098826 (T.J.P.), and R01NS100788 (Z.T.C.), R01NS114018 (Z.T.C.). The University of Texas STARS program (T.J.P.), the IBRO return home fellowship (P.B.-I.), and the IASP Early Career Research Grant (P.B.-I.). Z.T. Campbell, T.J. Price, and P. Barragan-Iglesias conceived the study. P. Barragan-Iglesias, J. Bryan de la Penã, T.-F. Lou, B. Black, R. Atmaramani, and N. Kunder performed

experiments. A. Wangzhou, P.R. Ray, and T. Shukla analyzed the sequencing data. Z.T. Campbell, T.J. Price, and P. Barragan-Iglesias wrote the manuscript. All authors approved the manuscript.

### Appendix A. Supplemental digital content

Supplemental digital content associated with this article can be found online at <http://links.lww.com/PAIN/B258> and <http://links.lww.com/PAIN/B259>.

### Article history:

Received 14 October 2020

Received in revised form 30 December 2020

Accepted 4 January 2021

Available online 11 January 2021

### References

- Amara SG, Jonas V, Rosenfeld MG, Ong ES, Evans RM. Alternative RNA processing in calcitonin gene expression generates mRNAs encoding different polypeptide products. *Nature* 1982;298:240–4.
- Andreev DE, O'Connor PB, Fahey C, Kenny EM, Terenin IM, Dmitriev SE, Cormican P, Morris DW, Shatsky IN, Baranov PV. Translation of 5' leaders is pervasive in genes resistant to eIF2 repression. *Elife* 2015;4:e03971.
- Avona A, Burgos-Vega C, Burton MD, Akopian AN, Price TJ, Dussor G. Dural calcitonin gene-related peptide produces female-specific responses in rodent migraine models. *J Neurosci* 2019;39:4323–31.
- Babendure JR, Babendure JL, Ding JH, Tsien RY. Control of mammalian translation by mRNA structure near caps. *RNA* 2006;12:851–61.
- Baird TD, Palam LR, Fusakio ME, Willy JA, Davis CM, McClintick JN, Anthony TG, Wek RC. Selective mRNA translation during eIF2 phosphorylation induces expression of IBTKalpha. *Mol Biol Cell* 2014;25:1686–97.
- Baliu-Pique M, Jusek G, Holzmann B. Neuroimmunological communication via CGRP promotes the development of a regulatory phenotype in TLR4-stimulated macrophages. *Eur J Immunol* 2014;44:3708–16.
- Bao Y, Gao Y, Yang L, Kong X, Yu J, Hou W, Hua B. The mechanism of μ-opioid receptor (MOR)-TRPV1 crosstalk in TRPV1 activation involves morphine anti-nociception, tolerance and dependence. *Channels (Austin)* 2015;9:235–43.
- Barragán-Iglesias P, de la pena J, Lou T, Loerch S, Kunder N, Shukla T, Basavarajappa L, Song J, Megat S, Moy J, Wangzhou A, Ray P, Shepherd J, Kenneth H, Steward O, Price T, Campbell Z. Intercellular Arc signaling regulates vasodilation. *bioRxiv* 2020. doi: 10.1101/2020.08.13.250209.
- Basbaum AI, Bautista DM, Scherrer G, Julius D. Cellular and molecular mechanisms of pain. *Cell* 2009;139:267–84.
- Beier H, Grimm M. Misreading of termination codons in eukaryotes by natural nonsense suppressor tRNAs. *Nucleic Acids Res* 2001;29:4767–82.
- Benemei S, Nicoletti P, Capone JG, Geppetti P. CGRP receptors in the control of pain and inflammation. *Curr Opin Pharmacol* 2009;9:9–14.
- Bhave G, Hu H-J, Glauner KS, Zhu W, Wang H, Brasier DJ, Oxford GS, Gereau RW. Protein kinase C phosphorylation sensitizes but does not activate the capsaicin receptor transient receptor potential vanilloid 1 (TRPV1). *Proc Natl Acad Sci U S A* 2003;100:12480–5.
- Black BJ, Atmaramani R, Kumaraju R, Plagens S, Romero-Ortega M, Dussor G, Price TJ, Campbell ZT, Pancrazio JJ. Adult mouse sensory neurons on microelectrode arrays exhibit increased spontaneous and stimulus-evoked activity in the presence of interleukin-6. *J Neurophysiol* 2018;120:1374–85.
- Bogen O, Alessandri-Haber N, Chu C, Gear RW, Levine JD. Generation of a pain memory in the primary afferent nociceptor triggered by PKCε activation of CPEB. *J Neurosci* 2012;32:2018–26.
- Cajigas IJ, Tushev G, Will TJ, tom Dieck S, Fuerst N, Schuman EM. The local transcriptome in the synaptic neuropil revealed by deep sequencing and high-resolution imaging. *Neuron* 2012;74:453–66.
- Calvo SE, Pagliarini DJ, Mootha VK. Upstream open reading frames cause widespread reduction of protein expression and are polymorphic among humans. *Proc Natl Acad Sci U S A* 2009;106:7507–12.

- [17] Chaplan SR, Bach FW, Pogrel JW, Chung JM, Yaksh TL. Quantitative assessment of tactile allodynia in the rat paw. *J Neurosci Methods* 1994; 53:55–63.
- [18] Chen J, Brunner AD, Cogan JZ, Nunez JK, Fields AP, Adamson B, Itzhak DN, Li JY, Mann M, Leonetti MD, Weissman JS. Pervasive functional translation of noncanonical human open reading frames. *Science* 2020; 367:1140–6.
- [19] Chew G-L, Pauli A, Schier AF. Conservation of uORF repressiveness and sequence features in mouse, human and zebrafish. *Nat Commun* 2016; 7:11663.
- [20] Chikumi H, Vázquez-Prado J, Servitja J-M, Miyazaki H, Gutkind JS. Potent activation of RhoA by  $\alpha$ q and Gq-coupled receptors. *J Biol Chem* 2002;277:27130–4.
- [21] Costa-Mattioli M, Sossin WS, Klann E, Sonenberg N. Translational control of long-lasting synaptic plasticity and memory. *Neuron* 2009;61: 10–26.
- [22] Dabrowski M, Bukowy-Bieryllo Z, Zietkiewicz E. Translational readthrough potential of natural termination codons in eucaryotes—The impact of RNA sequence. *RNA Biol* 2015;12:950–8.
- [23] Dunn JG, Foo CK, Belletier NG, Gavis ER, Weissman JS. Ribosome profiling reveals pervasive and regulated stop codon readthrough in *Drosophila melanogaster*. *Elife* 2013;2:e01179.
- [24] Eftekhari S, Salvatore CA, Johansson S, Chen TB, Zeng Z, Edvinsson L. Localization of CGRP, CGRP receptor, PACAP and glutamate in trigeminal ganglion. Relation to the blood-brain barrier. *Brain Res* 2015; 1600:93–109.
- [25] Eftekhari S, Warfvinge K, Blixt FW, Edvinsson L. Differentiation of nerve fibers storing CGRP and CGRP receptors in the peripheral trigeminovascular system. *J Pain* 2013;14:1289–303.
- [26] Ferrari LF, Bogen O, Levine JD. Role of nociceptor  $\alpha$ CaMKII in transition from acute to chronic pain (hyperalgesic priming) in male and female rats. *J Neurosci* 2013;33:11002–11.
- [27] Firth AE, Brierley I. Non-canonical translation in RNA viruses. *J Gen Virol* 2012;93:1385–409.
- [28] Franco-Cereceda A, Henke H, Lundberg JM, Petermann JB, Hokfelt T, Fischer JA. Calcitonin gene-related peptide (CGRP) in capsaicin-sensitive substance P-immunoreactive sensory neurons in animals and man: distribution and release by capsaicin. *Peptides* 1987;8:399–410.
- [29] Gao X, Wan J, Liu B, Ma M, Shen B, Qian SB. Quantitative profiling of initiating ribosomes in vivo. *Nat Methods* 2015;12:147–53.
- [30] Géranton SM, Jiménez-Díaz L, Torsney C, Tochiki KK, Stuart SA, Leith JL, Lumb BM, Hunt SP. A rapamycin-sensitive signaling pathway is essential for the full expression of persistent pain states. *J Neurosci* 2009; 29:15017–27.
- [31] Gibson DG, Smith HO, Hutchison CA, Venter JC, Merryman C. Chemical synthesis of the mouse mitochondrial genome. *Nat Methods* 2010;7: 901–3.
- [32] Gibson SJ, Polak JM, Gaiad A, Hamid QA, Kar S, Jones PM, Denny P, Legon S, Amara SG, Craig RK. Calcitonin gene-related peptide messenger RNA is expressed in sensory neurones of the dorsal root ganglia and also in spinal motoneurons in man and rat. *Neurosci Lett* 1988;91:283–8.
- [33] Gingras AC, Raught B, Gygi SP, Niedzwiecka A, Miron M, Burley SK, Polakiewicz RD, Wyslouch-Cieszyńska A, Aebersold R, Sonenberg N. Hierarchical phosphorylation of the translation inhibitor 4E-BP1. *Genes Dev* 2001;15:2852–64.
- [34] Glusman G, Caballero J, Robinson M, Kutlu B, Hood L. Optimal scaling of digital transcriptsomes. *PLoS One* 2013;8:e77885.
- [35] Hargreaves K, Dubner R, Brown F, Flores C, Joris J. A new and sensitive method for measuring thermal nociception in cutaneous hyperalgesia. *PAIN* 1988;32:77–88.
- [36] Hinnebusch AG. Gene-specific translational control of the yeast GCN4 gene by phosphorylation of eukaryotic initiation factor 2. *Mol Microbiol* 1993;10:215–23.
- [37] Hornstein N, Torres D, Das Sharma S, Tang G, Canoll P, Sims PA. Ligation-free ribosome profiling of cell type-specific translation in the brain. *Genome Biol* 2016;17:149.
- [38] Huth ME, Ricci AJ, Cheng AG. Mechanisms of aminoglycoside ototoxicity and targets of hair cell protection. *Int J Otolaryngol* 2011;2011:937861.
- [39] Ingolia NT. Genome-wide translational profiling by ribosome footprinting. *Methods Enzymol* 2010;470:119–42.
- [40] Ingolia NT, Brar GA, Stern-Ginossar N, Harris MS, Talhouarne GJ, Jackson SE, Wills MR, Weissman JS. Ribosome profiling reveals pervasive translation outside of annotated protein-coding genes. *Cell Rep* 2014;8:1365–79.
- [41] Ingolia NT, Ghaemmaghami S, Newman JR, Weissman JS. Genome-wide analysis in vivo of translation with nucleotide resolution using ribosome profiling. *Science* 2009;324:218–23.
- [42] Ingolia NT, Lareau LF, Weissman JS. Ribosome profiling of mouse embryonic stem cells reveals the complexity and dynamics of mammalian proteomes. *Cell* 2011;147:789–802.
- [43] Jiménez-Díaz L, Géranton SM, Passmore GM, Leith JL, Fisher AS, Berliocchi L, Sivasubramaniam AK, Sheasby A, Lumb BM, Hunt SP. Local translation in primary afferent fibers regulates nociception. *PLoS One* 2008;3:e1961.
- [44] Kaur C, Kumar M, Patankar S. Messenger RNAs with large numbers of upstream open reading frames are translated via leaky scanning and reinitiation in the asexual stages of *Plasmodium falciparum*. *Parasitology* 2020;147:1100–13.
- [45] Kilo S, Harding-Rose C, Hargreaves KM, Flores CM. Peripheral CGRP release as a marker for neurogenic inflammation: a model system for the study of neuropeptide secretion in rat paw skin. *PAIN* 1997;73:201–7.
- [46] Kopczyński JB, Raff AC, Bonner JJ. Translational readthrough at nonsense mutations in the HSF1 gene of *Saccharomyces cerevisiae*. *Mol Gen Genet* 1992;234:369–78.
- [47] Kozak M. The scanning model for translation: an update. *J Cell Biol* 1989; 108:229–41.
- [48] de la Pena JBI, Song JJ, Campbell ZT. RNA control in pain: blame it on the messenger. *Wiley Interdiscip Rev RNA* 2019;10:e1546.
- [49] Lennerz JK, Ruhle V, Ceppa EP, Neuhuber WL, Bunnett NW, Grady EF, Messlinger K. Calcitonin receptor-like receptor (CLR), receptor activity-modifying protein 1 (RAMP1), and calcitonin gene-related peptide (CGRP) immunoreactivity in the rat trigeminovascular system: differences between peripheral and central CGRP receptor distribution. *J Comp Neurol* 2008;507:1277–99.
- [50] Li Z, Dong X, Wang Z, Liu W, Deng N, Ding Y, Tang L, Hla T, Zeng R, Li L, Wu D. Regulation of PTEN by Rho small GTPases. *Nat Cell Biol* 2005;7:399–404.
- [51] Loerch S, De la Peña JB, Song Pancrazio JJJ, Price TJ, Campbell ZT. Translational controls in pain. In: Sossin W, editor. *The Oxford Handbook of Neuronal Protein Synthesis*. Oxford, United Kingdom: Oxford University Press, 2019. p. 1–26.
- [52] Lopez-Novoa JM, Quiros Y, Vicente L, Morales AI, Lopez-Hernandez FJ. New insights into the mechanism of aminoglycoside nephrotoxicity: an integrative point of view. *Kidney Int* 2011;79:33–45.
- [53] Malin SA, Davis BM, Koerber HR, Reynolds IJ, Albers KM, Molliver DC. Thermal nociception and TRPV1 function are attenuated in mice lacking the nucleotide receptor P2Y2. *PAIN* 2008;138:484–96.
- [54] Megat S, Ray PR, Moy JK, Lou TF, Barragan-Iglesias P, Li Y, Pradhan G, Wangzhou A, Ahmad A, Burton MD, North RY, Dougherty PM, Khoutorsky A, Sonenberg N, Webster KR, Dussor G, Campbell ZT, Price TJ. Nociceptor translational profiling reveals the regulator-rag GTPase complex as a critical generator of neuropathic pain. *J Neurosci* 2019;39:393–411.
- [55] Megat S, Ray PR, Tavares-Ferreira D, Moy JK, Sankaranarayanan I, Wangzhou A, Fang Lou T, Barragan-Iglesias P, Campbell ZT, Dussor G, Price TJ. Differences between dorsal root and trigeminal ganglion nociceptors in mice revealed by translational profiling. *J Neurosci* 2019; 39:6829–47.
- [56] Melemedjian OK, Asiedu MN, Tillu DV, Peebles KA, Yan J, Ertz N, Dussor GO, Price TJ. IL-6- and NGF-induced rapid control of protein synthesis and nociceptive plasticity via convergent signaling to the eIF4F complex. *J Neurosci* 2010;30:15113–23.
- [57] Melemedjian OK, Tillu DV, Moy JK, Asiedu MN, Mandell EK, Ghosh S, Dussor G, Price TJ. Local translation and retrograde axonal transport of CREB regulates IL-6-induced nociceptive plasticity. *Mol Pain* 2014;10: 45.
- [58] Moriyama T, Higashi T, Togashi K, Iida T, Segi E, Sugimoto Y, Tominaga T, Narumiya S, Tominaga M. Sensitization of TRPV1 by EP1 and IP reveals peripheral nociceptive mechanism of prostaglandins. *Mol Pain* 2005;1:3.
- [59] Moy JK, Khoutorsky A, Asiedu MN, Black BJ, Kuhn JL, Barragan-Iglesias P, Megat S, Burton MD, Burgos-Vega CC, Melemedjian OK, Boitano S, Vagner J, Gkogkas CG, Pancrazio JJ, Mogil JS, Dussor G, Sonenberg N, Price TJ. The MNK-eIF4E signaling axis contributes to injury-induced nociceptive plasticity and the development of chronic pain. *J Neurosci* 2017;37:7481–99.
- [60] Ohta T, Ikemi Y, Murakami M, Imagawa T, Otsuguro K, Ito S. Potentiation of transient receptor potential V1 functions by the activation of metabotropic 5-HT receptors in rat primary sensory neurons. *J Physiol* 2006;576:809–22.
- [61] Reichling DB, Levine JD. Critical role of nociceptor plasticity in chronic pain. *Trends Neurosci* 2009;32:611–8.
- [62] Rodriguez CM, Chun SY, Mills RE, Todd PK. Translation of upstream open reading frames in a model of neuronal differentiation. *BMC Genomics* 2019;20:391.



- [63] Rosenfeld MG, Mermod JJ, Amara SG, Swanson LW, Sawchenko PE, Rivier J, Vale WW, Evans RM. Production of a novel neuropeptide encoded by the calcitonin gene via tissue-specific RNA processing. *Nature* 1983;304:129–35.
- [64] Rozenbaum M, Rajman M, Rishal I, Koppel I, Koley S, Medzihradzky KF, Oses-Prieto JA, Kawaguchi R, Amieux PS, Burlingame AL, Coppola G, Fainzilber M. Translational regulation in neuronal injury and axon regrowth. *eNeuro* 2018;5. doi:10.1523/ENEURO.0276-17.2018.
- [65] Russell FA, King R, Smillie SJ, Kodji X, Brain SD. Calcitonin gene-related peptide: physiology and pathophysiology. *Physiol Rev* 2014;94:1099–142.
- [66] Salzer I, Gantumur E, Yousuf A, Boehm S. Control of sensory neuron excitability by serotonin involves 5HT<sub>2C</sub> receptors and Ca<sup>2+</sup>-activated chloride channels. *Neuropharmacology* 2016;110:277–86.
- [67] Schmidt RL, Simonovic M. Synthesis and decoding of selenocysteine and human health. *Croat Med J* 2012;53:535–50.
- [68] Schnizler K, Shutov LP, Van Kanegan MJ, Merrill MA, Nichols B, McKnight GS, Strack S, Hell JW, Usachev YM. Protein kinase A anchoring via AKAP150 is essential for TRPV1 modulation by forskolin and prostaglandin E<sub>2</sub> in mouse sensory neurons. *J Neurosci* 2008;28:4904–17.
- [69] Schönwasser DC, Marais RM, Marshall CJ, Parker PJ. Activation of the mitogen-activated protein kinase/extracellular signal-regulated kinase pathway by conventional, novel, and atypical protein kinase C isoforms. *Mol Cell Biol* 1998;18:790–8.
- [70] Sculptoreanu A, Aura Kullmann F, de Groat WC. Neurokinin 2 receptor-mediated activation of protein kinase C modulates capsaicin responses in DRG neurons from adult rats. *Eur J Neurosci* 2008;27:3171–81.
- [71] Sendoel A, Dunn JG, Rodriguez EH, Naik S, Gomez NC, Hurwitz B, Levorse J, Dill BD, Schramek D, Molina H, Weissman JS, Fuchs E. Translation from unconventional 5' start sites drives tumour initiation. *Nature* 2017;541:494–9.
- [72] Spealman P, Naik AW, May GE, Kuersten S, Freeberg L, Murphy RF, McManus J. Conserved non-AUG uORFs revealed by a novel regression analysis of ribosome profiling data. *Genome Res* 2018;28:214–22.
- [73] Springer J, Geppetti P, Fischer A, Groneberg DA. Calcitonin gene-related peptide as inflammatory mediator. *Pulm Pharmacol Ther* 2003;16:121–30.
- [74] Starck SR, Tsai JC, Chen K, Shodiya M, Wang L, Yahiro K, Martins-Green M, Shastri N, Walter P. Translation from the 5' untranslated region shapes the integrated stress response. *Science* 2016;351:aad3867.
- [75] Sugiuar T. TRPV1 function in mouse colon sensory neurons is enhanced by metabotropic 5-hydroxytryptamine receptor activation. *J Neurosci* 2004;24:9521–30.
- [76] Tang H-B, Inoue A, Oshita K, Nakata Y. Sensitization of vanilloid receptor 1 induced by bradykinin via the activation of second messenger signaling cascades in rat primary afferent neurons. *Eur J Pharmacol* 2004;498:37–43.
- [77] Tappe-Theodor A, Constantin CE, Tegeder I, Lechner SG, Langeslag M, Lepczynsky P, Wirotanseng RI, Kurejova M, Agarwal N, Nagy G, Todd A, Wettschreck N, Offermanns S, Kress M, Lewin GR, Kuner R. G $\alpha$ (q/11) signaling tonically modulates nociceptor function and contributes to activity-dependent sensitization. *PAIN* 2012;153:184–96.
- [78] Uttam S, Wong C, Amorim IS, Jafarnejad SM, Tansley SN, Yang J, Prager-Khoutorsky M, Mogil JS, Gkogkas CG, Khoutorsky A. Translational profiling of dorsal root ganglia and spinal cord in a mouse model of neuropathic pain. *Neurobiol Pain* 2018;4:35–44.
- [79] de Vries T, MaassenVanDenBrink A. CGRP-targeted antibodies in difficult-to-treat migraine. *Nat Rev Neurol* 2019;15:688–9.
- [80] Waldo GL, Boyer JL, Morris AJ, Harden TK. Purification of an AIF4- and G-protein beta gamma-subunit-regulated phospholipase C-activating protein. *J Biol Chem* 1991;266:14217–25.
- [81] Wirotanseng LN, Kuner R, Tappe-Theodor A. Gq rather than G11 preferentially mediates nociceptor sensitization. *Mol Pain* 2013;9:54.
- [82] Xu Y, Poggio M, Jin HY, Shi Z, Forester CM, Wang Y, Stumpf CR, Xue L, Devericks E, So L, Nguyen HG, Griselin A, Gordan JD, Umetsu SE, Reich SH, Worland ST, Asthana S, Barna M, Webster KR, Cunningham JT, Ruggero D. Translation control of the immune checkpoint in cancer and its therapeutic targeting. *Nat Med* 2019;25:301–11.
- [83] Young SK, Wek RC. Upstream open reading frames differentially regulate gene-specific translation in the integrated stress response. *J Biol Chem* 2016;291:16927–35.
- [84] Yousuf A, Klinger F, Schicker K, Boehm S. Nucleotides control the excitability of sensory neurons via two P2Y receptors and a bifurcated signaling cascade. *PAIN* 2011;152:1899–908.
- [85] Zhang H, Cang C-L, Kawasaki Y, Liang L-L, Zhang Y-Q, Ji R-R, Zhao Z-Q. Neurokinin-1 receptor enhances TRPV1 activity in primary sensory neurons via PKC: a novel pathway for heat hyperalgesia. *J Neurosci* 2007;27:12067–77.